

The Role of Graphene in Enhancing the Material Properties of Thermosetting Polymers

Maxime Vassaux, Robert C. Sinclair, Robin A. Richardson, James L. Suter, and Peter V. Coveney*

Graphene continues to attract considerable attention from the materials science community through its potential for improving the mechanical properties of polymer thermosets, yet there remains considerable uncertainty over the underlying mechanisms. The effect of introducing graphene sheets to a typical thermosetting polymer network on mechanical behaviour is explored here through concurrently coupling molecular dynamics with a finite element solver. In this multiscale approach, Graphene is observed to act in two ways: as passive microscopic defects, dispersing crack propagation (high deformation); and as active geometric constraints, impeding polymer conformational changes (low deformation). By contrast, single-scale atomistic simulations alone predict little measurable difference in the properties of the graphene-enhanced epoxy resins as compared with the pure polymer case. The multiscale model predicts that epoxy resins reinforced with graphene nanoparticles exhibit enhanced overall elastoplastic properties, reducing strain energy dissipation by up to 70%. Importantly, this is only observed when taking into account the complex boundary conditions, mainly involving shear, arising from coupling physics on length scales separated by five orders of magnitude. The approach herein clearly highlights a novel role of graphene nanoparticles in actively constraining the surrounding polymer matrix, impeding local dissipative mechanisms, and resisting shear deformation.


Graphene exhibits some astonishing physical properties, and it is mechanically known to have tremendous strength and stiffness, but pure graphene has little chance of being employed as a structural material by itself. Manufacturing single layers of graphene at large scale is a major challenge.^[1–3] One popular

technique to exploit the mechanical properties of graphene industrially is to combine it with polymer to create nanocomposites. In this paper, we concentrate on epoxy derived nanocomposites, which are of considerable importance in the aerospace and automotive industries. Epoxy resins are known to be brittle,^[4] but are found to display improved toughness when enhanced with graphene nanoparticles.^[5–8] However, underlying mechanisms explaining the enhancement of the properties of these nanocomposites remain poorly understood. So far, two different, potentially complementary, theories have been formulated in this regard: crack deflection^[6,7] and microcrack dispersion.^[9] Furthermore, graphene-based enhancement of the intermediate elastoplastic properties of epoxy resins, such as yield and hardening, are rarely addressed experimentally. The response of epoxy resins subject to tensile loading transitions from elastic to brittle fracture instantly. These intermediate properties are therefore not observable through standard engineering testing procedures. However, yield and hardening are highly

relevant in the day to day use of structural components. They express the material's aptitude to store and return strain energy, under cyclic loading, while remaining functional. Our work is able to elucidate these issues for the first time, as we now show.

Density functional theory and molecular dynamics are the tools of choice of many academic materials scientists concerned with chemical fidelity, but ab initio physical models are unfeasible in applications beyond the smallest scales (i.e., the nanoscale). Consequently, these methods overlook the multiscale nature of most real-world material properties. Their properties emerge from the geometrical and structural complexity at engineering scales, which induce a heterogeneous mixture of local mechanical states triggering specific micromechanisms. Current attempts to capture multiscale complexity and explore the material properties of a system of atoms most often involve ad hoc assumptions,^[10] in the form of constitutive modeling. Such approaches omit peculiarities of the stress–strain response of a newly formulated material. However, modern high-performance computational resources, coupled with sophisticated multiscale modeling techniques, enable us

Dr. M. Vassaux, R. C. Sinclair, Dr. R. A. Richardson, Dr. J. L. Suter, Prof. P. V. Coveney
Centre for Computational Sciences
University College London
20 Gordon Street, London, WC1H 0AJ, United Kingdom
E-mail: p.v.coveney@ucl.ac.uk

 The ORCID identification number(s) for the author(s) of this article can be found under <https://doi.org/10.1002/adts.201800168>

© 2019 The Authors. Published by WILEY-VCH Verlag GmbH & Co. KGaA, Weinheim. This is an open access article under the terms of the Creative Commons Attribution License, which permits use, distribution and reproduction in any medium, provided the original work is properly cited.

The copyright line was changed 28 March 2019 after initial publication.

DOI: [10.1002/adts.201800168](https://doi.org/10.1002/adts.201800168)

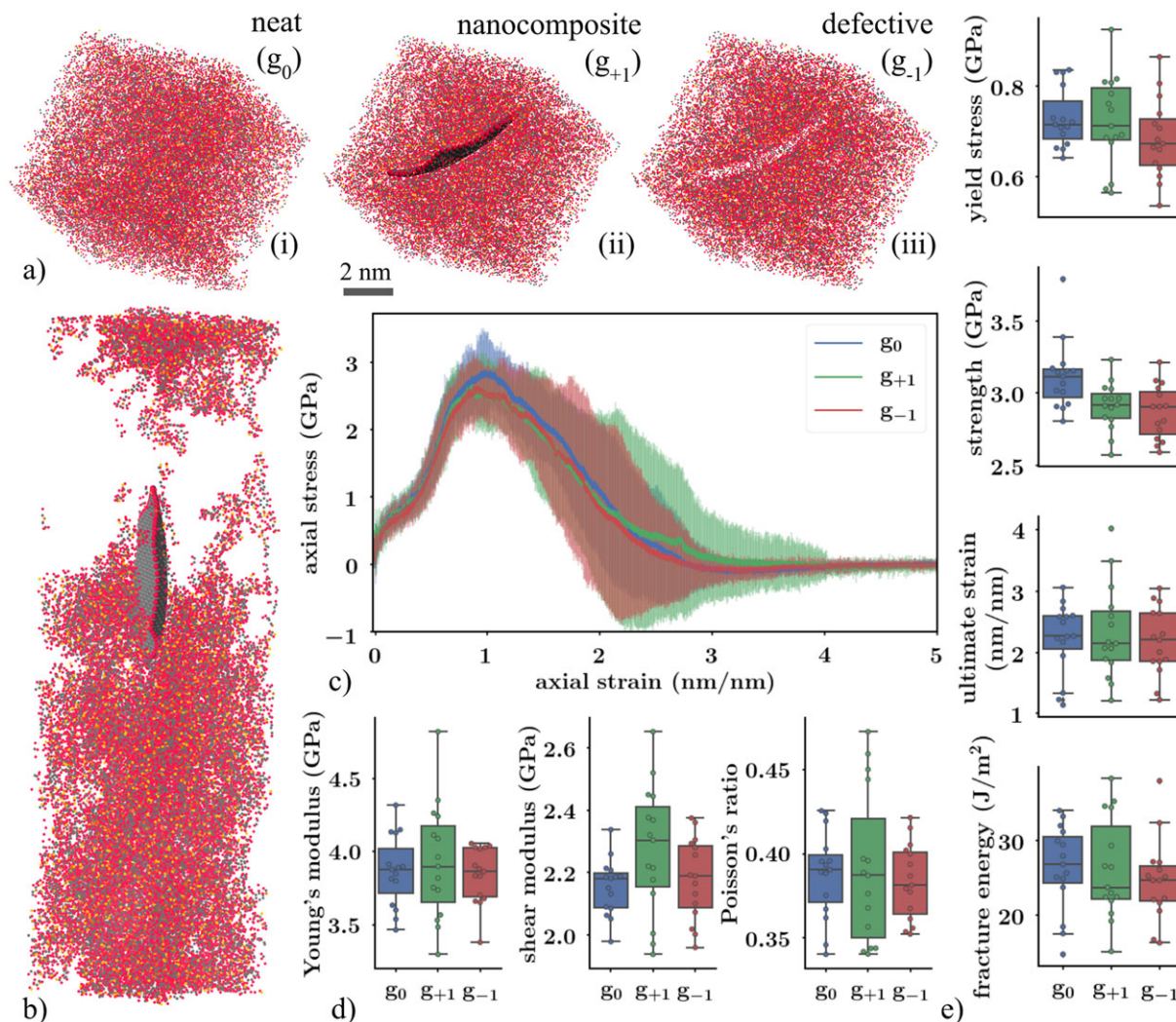


Figure 1. a) The structure of three atomistic systems after equilibration: i) neat epoxy (g_0), ii) nanocomposite epoxy (g_{+1}) and iii) defective epoxy (g_{-1}). The structure of the polymer network in the (g_{+1}) and (g_{-1}) systems is identical. b) The atomistic structure of the (g_{+1}) system, strained in the vertical direction at +200%. The graphene sheet has aligned with the direction of stretching and resides in the location of void growth, falling short of bridging the growing crack. c) The evolution of the axial stress versus the axial strain in the direction of stretching in all three systems. The continuous line is the mean over 15 replicas, and the shaded area is the 95% confidence interval (2σ). The three systems display a very similar sequence of behaviors: elasticity, yield, hardening, softening and, finally, failure. The elastic regime is limited to a small part of the strain amplitude. Quantification d) of elastic, and e) of plastic and fracture mechanical properties for all three systems, shown via box plots of the distribution for each ensemble of replicas. The shear modulus is the only property being enhanced by the presence of graphene, while other properties remain mostly unchanged or, in some cases, diminished, for example, the fracture properties (strength, fracture energy).

to conduct high fidelity predictive modeling and simulation at scales relevant to mechanical engineering.^[11–13]

We begin with an investigation of the properties of graphene–epoxy nanocomposites at the atomistic scale by performing extensive testing of the nanocomposite properties from elastic to failure regimes. Remarkably, the expected enhancement in the toughness of the epoxy resin through the addition of graphene 2D nanoparticles is found to be negligible in such atomistic simulations. On the basis of these atomistic simulations, we characterize the complex interaction between a single 2D nanoparticle and the surrounding crosslinked network. We then explore the properties of the nanocomposite at the engineering scale through a concurrent multiscale approach, seeking new

behaviors that could emerge from the coupling of mechanisms at different scales. For the first time, we simulated large scale high-velocity “drop-weight” impact tests on a thin (5 mm) shell, while preserving chemical specificity of the material. This results in the nanocomposite facing a combination of 3D local mechanical states as well as a transient cyclic load characteristic of engineering applications such as those found in industrial turbines, engines, and sports appliances. This complex testing setup offers us new insights into the enhanced material properties caused by the addition of graphene into epoxy resins.

At the atomistic scale, we explore the interactions of single sheets of graphene with the surrounding epoxy resin. We compare three $8\text{nm} \times 8\text{nm} \times 8\text{nm}$ systems (see Figure 1a): i) neat

epoxy (g_0), ii) 3.5% weight ratio nanocomposite epoxy (g_{+1}), and iii) defective epoxy (g_{-1}), identical to (g_{+1}) after removal of graphene. These computer-based systems are subject to uniaxial and shear loading to measure their elastic properties. Uniaxial loading is applied until failure to exhibit plastic and fracture properties. The nanocomposite systems embed a single hexagonal graphene nanoparticle approximately 6 nm wide. For statistical relevance, an ensemble of 15 replicas with identical density and crosslinking degree, differing in their initial atomistic structure, are tested.^[14] The analysis is performed with molecular dynamics simulations using LAMMPS^[15] and the ReaxFF force field.^[16] The epoxy resins consist of tetraglycidyl methylene dianiline precursor and polyetheramine curing agent, reaching a crosslinking degree of 92% on average. A tetrafunctional thermoset with high degree of crosslinking is assumed to provide higher confinement of the 2D nanoparticles, thereby recruiting more efficiently their mechanical properties, via geometrical constraints. Graphene particles are added to the polymer precursors, prior to the curing phase. Full details on the simulation of the cure of the nanocomposite systems, equilibration and mechanical deformation via molecular dynamics, as well as verification and validation against experiments, can be found in the Supporting Information.

On average, the impact of graphene at the nanoscale (g_{+1}) is small (see Figure 1). The results include loading in three orthogonal directions presented in order to limit the influence of the anisotropy induced by the 2D nanoparticle on the mean. Nevertheless, because of the induced anisotropy, the variability of the properties of the nanocomposites is higher than that of the neat epoxy resin.

The nanocomposite replicas show an increase in shear modulus of approximately 5%, while their strength and fracture energy follow the converse trend. A slightly enhanced resilience at extreme strains is observed during evolution of the uniaxial stress (see Figure 1b); nonetheless, the ultimate strain at the point of failure of the nanocomposite remains unchanged. Consequently, the reduced peak stress leads to lower amounts of dissipated energy, both on the order of a few percent.

Observing the structure of the stretched nanocomposite, the interaction between the sheet of graphene and the polymer strands appears minimal. As can be seen in the snapshot of the atomistic structure at 200% tensile strain presented in Figure 1a, the sheet is completely aligned with the load direction and resides where the void growth is localized. This is observed in all simulations, independent of the initial sheet orientation and loading direction. The sheet of graphene therefore does not provide any geometrical constraint to conformational changes. Furthermore, the 2D nanoparticle falls short of bridging the voids, and fails to pin the crack. Neither cohesion, attraction, or frictional forces emerging from the interaction with the polymer appear sufficient to resist the fracture of the polymer structure.

Conversely, the enhanced shear modulus might imply that, under pure shear that is a constant-volume strain, the graphene sheet acts as a flow constraint. The limited effect of the graphene sheet, solely influencing elastic properties, is consistent with the experimental work of ref. [17], who claimed that slippage at the interface between graphene and polymer matrices is observed at shear strains as low as 0.7%. In turn, at strains relevant to yield and failure (above 10%), neither direct interac-

tion nor force transfer would be expected at the graphene/epoxy interface.

These findings would appear to support the “microcracks” theory,^[9] in which the graphene acts as a precursor to void growth. Therefore, we explore to what extent the graphene sheet can be viewed as a defect. All simulations performed on the nanocomposite system were conducted again with the same polymer structure minus the atoms of the graphene sheet (g_{-1}). The atoms which have been removed leave an empty volume in the initial configuration of the polymer system (Figure 1).

The original (neat epoxy) shear modulus is immediately restored upon removal of the graphene sheet, highlighting the influence of the rigid, impenetrable inclusion previously opposing the local flow of the polymer. However, the altered fracture properties of the nanocomposite are preserved, leading us to infer that the true influence of the graphene sheet lies in the way it disrupts the surrounding network of interconnected polymer strands. Consequently, the most relevant property of graphene is its high surface area to weight ratio, rather than its outstanding strength and stiffness.

Having investigated the influence of a single sheet of graphene, we now simulate a macroscopic structure integrating the effect of a large number of them. Drawing on a novel application of the heterogeneous multiscale method^[18] to the inelastic behavior of amorphous materials,^[19] we simulated the behavior of a thin rectangular shell of epoxy nanocomposite of dimensions 150 mm × 100 mm × 5 mm for 0.2 ms. Our approach reduces this system to two significant scales. On the one hand, we include the atomistic scale characterized by several replicas of the molecular dynamics models (see Figure 1a). On the other hand, the continuum scale is described by a finite element mesh of the shell (Figure 2a) and a random distribution of neat and nanocomposite epoxy to achieve a given weight ratio.

While solving the continuum finite element model of the shell using the finite element library Deal.II,^[20] the stress is directly obtained from an ensemble of molecular dynamics simulations performed again with LAMMPS (see the Supporting Information for details) rather than from a phenomenological constitutive equation. The molecular dynamics simulations are performed on periodic and homogeneous systems of 8 nm × 8 nm × 8 nm and at strain rates allowing relaxation ($<0.1 \text{ ns}^{-1}$), enabling the assumption of time and space scale separation (see Figure S3, Supporting Information).

The shell of epoxy resin is subject to a high-velocity impact of 400 m s^{-1} at its centre, and is vertically supported at its lateral edges. The impactor is a rigid cylinder of 20-mm diameter applying a constant acceleration on the shell for $5 \mu\text{s}$. Different shell compositions are simulated: neat epoxy and a mixture of neat epoxy (g_0 , blue) and nanocomposite ($g_{+/-1}$, gray) to reach an overall 1% weight ratio (Figure 2a). The impacted shell oscillates freely after impact (Figure 2b), locally facing a mixture of low amplitude volumetric and constant-volume shear strain. Note that the shear component dominates over the volumetric component of the stress tensor throughout the experiment (Figure 2c).

The neat and nanocomposite shells receive comparable amounts of mechanical energy from the impact (left enclosed caption, Figure 2d). However, the neat epoxy shell faces a rapid and significant decrease of the total energy stored in the shell

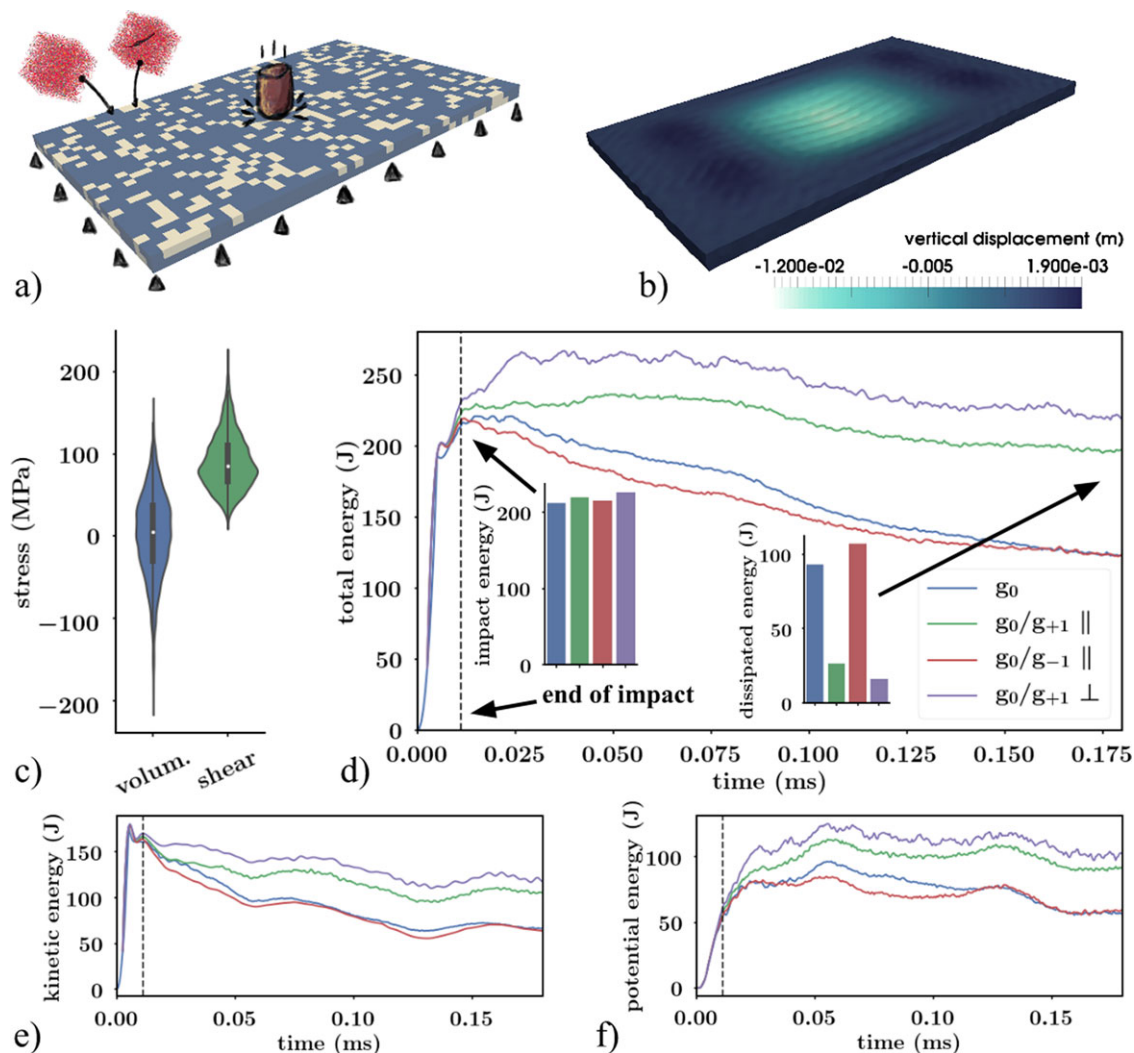


Figure 2. a) The finite element model of a shell is impacted vertically in its centre by a rigid cylinder travelling at 400 m s^{-1} . The edges of the shell are fixed. The shell is either composed entirely of neat epoxy (g_0) or a mixture of neat epoxy and nanocomposites/defective epoxy (g_0/g_{+1}), as in Figure 1. Each cell of the FE mesh is endowed with a system type according to a random spatial distribution of the g_0 (blue) and g_{+1} (gray) systems across the shell. b) The deformed shell 1.5×10^{-4} s after impact. The color indicates the amplitude of the vertical displacement. c) Violin plot of the distribution of the local stresses in the g_0/g_{+1} shell 1.5×10^{-4} s after impact, focusing on the volumetric (11-invariant) and the shear (von Mises) components of the stress tensor. Shear is the predominant local mechanical state in the shell in that snapshot and remains so during the entire impact test. Evolution of the d) total, e) potential, and f) kinetic energies in the shell during simulation. In addition to the neat epoxy (blue, g_0), three mixture configurations are tested: i) the neat epoxy is mixed with nanocomposite epoxy having all the sheets aligned in the plane of the shell (green, $g_0/g_{+1} \parallel$), ii) all the sheets are orthogonal to the plane of the shell (purple, $g_0/g_{+1} \perp$), and iii) with the defective epoxy having all the defects aligned in the plane of the shell (red, $g_0/g_{-1} \parallel$). The dashed black line indicates the end of contact between the shell and the cylindrical impactor. The quantification of the total energy transferred from the impactor to the shell is shown in the left insert, while the total energy dissipation at the end of the simulation is found in the right insert in (d). The g_0/g_{+1} shell is able to retain almost the entire impact elastic energy independently of the orientation of the sheet, while g_0 dissipates more than a third of the energy of impact. When the sheets are removed from these simulations (g_0/g_{-1}), the energy dissipation returns to that of the neat epoxy shell.

(Figure 2d). Both the kinetic and the potential energy are dissipated, which is accomplished entirely by the thermostat enforced at the atomistic scale. Note that the potential energy is comprised entirely of strain energy. In the meantime, the total energy in the nanocomposite shells hardly decreases after impact. This is observed independently of the orientation of the graphene sheets in the shell, whether the sheet is aligned with the shell ($g_0/g_{+1} \parallel$) or orthogonal to the shell ($g_0/g_{+1} \perp$). The final dissipated energy, measured as the difference between the peak and the end-of-test

total energy values (right enclosed caption, Figure 2d), shows a 300% energy dissipation increase between the nanocomposites and the neat epoxy. The stress amplitudes induced by the impact remain moderately low, below 0.2 GPa, therefore the energy dissipation is not related to fracture or void expansion. In turn, dissipation must be in the form of heat induced by friction. We conclude that the nanocomposites exhibit reduced structural conformational changes compared to their neat epoxy counterpart, accounting for the reduced hysteresis effect. When the graphene

sheets are removed (g_0/g_{-1} ||), the observed reduction of energy dissipation is entirely lost, and values similar to those of the neat epoxy shell are restored. Such observations challenge the microcrack theory, which treats graphene nanoparticles as merely passive inclusions.

Further inspection of local quantities reveals once again that force transfer to the graphene nanoparticles is minimal. The potential energy of the sheets at the end of the g_0/g_{+1} simulations is negligible, and has actually decreased ($-20 \text{ kcal mol}^{-1}$). The variation of the potential energy of the graphene represents on average 1% of the variation of the strain energy within the nanocomposite. The potential energy of the sheet does not depend on the local mechanical state of its surroundings (see Figure S7, Supporting Information). The stiffness of graphene therefore does not appear to be recruited by the polymer. This is consistent with the observation that force transfer occurs only at very low strain amplitudes as reported experimentally by ref. [17], especially in non-functionalized graphene sheets.

As active force transfer of nanoparticles appears to be irrelevant, we delve into passive mechanisms. Density profiles in the normal direction of the flake show that no specific reorganisation or densification of the polymer can be observed in the vicinity of the graphene (see Figure S8, Supporting Information). In turn, the 2D nanoparticle is not found to act as an impenetrable barrier during the cure of the polymer promoting the crystallisation of the polymer in its vicinity, unlike that reported by ref. [21] for thermoplastic polymers.

Although the potential energy in the graphene sheet remains low, the differences observed between the (g_0/g_{+1}) and the (g_0/g_{-1}) shells implies that the presence of graphene affects the global elastoplastic behavior of the shell. Drawing on the observed enhancements of the shear modulus at the atomistic level, and the predominance of shear stress in the impacted shell (Figure 2c), it appears that graphene is particularly efficient at enhancing the elasticity of the nanocomposite under constant-volume or shear strains. Constant-volume deformation maintains high levels of nanoconfinement, which has been shown to increase the influence of nanoparticles.^[22] This supports the concept that graphene acts as a barrier preventing conformational changes in the surrounding polymer upon loading. While not necessarily running contrary to predictions of the microcrack theory regarding fracture properties, it nonetheless confirms that graphene sheets have different effects on the epoxy nanocomposite depending on the amplitude and the type of mechanical stress undergone.

We have investigated the properties of graphene–epoxy nanocomposites using both a single-scale molecular dynamics approach and a multiscale approach which couples the atomistic description with a finite element representation at the continuum scale. Atomistic analysis of the nanocomposite reveals little difference in the responses between the neat and graphene-enhanced epoxy resins under uniaxial tension. The Young's modulus, Poisson's ratio, yield stress, hardening, and strength show surprising similarity in the two cases. We conclude from the atomistic simulations that a graphene nanoparticle embedded in a thermosetting polymer network acts primarily as a defect. The intrinsic properties of the graphene sheet, its stiffness and strength, are not transferred to the polymer network as a

whole. Interestingly, this mechanism is fundamentally different from that observed in thermoplastic nanocomposites, where polymer is absorbed on and tightly bound to the surface of the 2D nanoparticles,^[23] leading to consistent enhancement of the strength. Multiscale analysis^[19] of the nanocomposite uncovers enhanced elastic capabilities due to inclusion of graphene particles. At relatively low amplitude oscillations, the nanocomposite dissipates up to 70% less of the energy caused by the impact in the form of strain energy. In the case of uniaxial tension, the properties of the epoxy resin appear largely unchanged by the presence of graphene. In contrast, under 3D anisotropic loading conditions—that crucially only arise from the multiscale treatment of the system—the presence of graphene is in fact observed to extend the elastic regime and to reduce hysteresis effects. This has important implications for materials simulation, in which only single scale uniaxial tension is considered. Graphene particles act as a nanoscale constraint, preventing conformational changes within the polymer network, leading to enhancement of the shear modulus and strain energy restitution within the nanocomposite. These discoveries about the role of graphene in thermosetting plastics cannot be inferred either from microcrack theory or from atomistic simulations alone. By applying our multiscale method to graphene–epoxy nanocomposites, we have uncovered the mechanisms responsible for materials behavior relevant to a wide range of industrial applications, from tennis rackets to industrial turbines. Further developments of this modeling approach are now underway to allow us to describe fracture in this multiscale context, while the computational expense of the method is being reduced by the incorporation of surrogate models.

Supporting Information

Supporting Information is available from the Wiley Online Library or from the author.

Acknowledgements

The authors acknowledge funding support from the European Union's Horizon 2020 research and innovation programme under grant agreement 223979 (ComPat project, www.compat-project.eu) and 800925 (VECMA project, www.vecma.eu), and from the U.K. Consortium on Mesoscale Engineering Sciences (UKCOMES, www.ukcomes.org), EPSRC reference EP/L00030X/1. The authors are grateful to the Poznań Supercomputing and Networking Center for access to the Eagle supercomputer, the CYFRONET AGH Academic Computer Centre in Krakow for access to the Prometheus supercomputer, and the Leibniz Supercomputing Centre for providing access to SuperMUC. The authors also made use of ARCHER, the U.K.'s National High Performance Computing Service, funded by the Office of Science and Technology through the EPSRC's High-End Computing Programme. The authors thank Dr. David Tilbrook of Hexcel, Ltd., for his advice on the choice of epoxy resins for study and ways of building molecular models of these polymers.

Conflict of Interest

The authors declare no conflict of interest.

Keywords

material properties, multiscale modeling, nanocomposite, polymer thermostat, single-layer graphene

Received: October 29, 2018

Revised: January 24, 2019

Published online: February 18, 2019

-
- [1] X. Wang, H. You, F. Liu, M. Li, L. Wan, S. Li, Q. Li, Y. Xu, R. Tian, Z. Yu, D. Xiang, J. Cheng, *Chem. Vap. Deposition* **2009**, *15*, 53.
- [2] R. Sinclair, J. L. Suter, P. V. Coveney, *Adv. Mater.* **2018**, *30*, 1705791.
- [3] R. Sinclair, J. L. Suter, P. V. Coveney, accepted for publication **2018**.
<https://doi.org/10.1039/c8cp07796g>
- [4] A. C. Garg, Y.-W. Mai, *Compos. Sci. Technol.* **1988**, *31*, 179.
- [5] H. Kim, A. A. Abdala, C. W. Macosko, *Macromolecules* **2010**, *43*, 6515.
- [6] S. Shadlou, B. Ahmadi-Moghadam, F. Taheri, *Mater. Des.* **2014**, *59*, 439.
- [7] I. Zaman, T. T. Phan, H.-C. Kuan, Q. Meng, L. T. Bao La, L. Luong, O. Youssf, J. Ma, *Polymer* **2011**, *52*, 1603.
- [8] M. Naebe, J. Wang, A. Amini, H. Khayyam, N. Hameed, L. H. Li, Y. Chen, B. L. Fox, *Sci. Rep.*, **2014**, *4*, 4375.
- [9] Y. T. Park, Y. Qian, C. Chan, T. Suh, M. G. Nejjad, C. W. Macosko, A. Stein, *Adv. Funct. Mater.* **2015**, *25*, 575.
- [10] J. L. Bouvard, D. K. Ward, D. Hossain, S. Nouranian, E. B. Marin, M. F. Horstemeyer, *J. Eng. Mater. Technol.* **2009**, *131*, 041206.
- [11] A. Hoekstra, B. Chopard, P. Coveney, *Phil. Trans. R. Soc. A* **2014**, *372*, 20130377.
- [12] S. Alowayyed, D. Groen, P. V. Coveney, A. G. Hoekstra, *Journal of Comput. Sci.* **2017**, *22*, 15.
- [13] S. Alowayyed, T. Piontek, J. L. Suter, O. Hoenen, D. Groen, O. Luk, B. Bosak, P. Kopta, K. Kurowski, O. Perks, K. Brabazon, V. Jancauskas, D. Coster, P. V. Coveney, A. G. Hoekstra, *Future Gener. Comput. Syst.* **2019**, *91*, 335.
- [14] P. V. Coveney, S. Wan, *Phys. Chem. Chem. Phys.* **2016**, *18*, 30236.
- [15] S. Plimpton, *J. Comput. Phys.* **1995**, *117*, 1.
- [16] H. M. Aktulga, J. C. Fogarty, S. A. Pandit, A. Y. Grama, *Parallel Comput.* **2012**, *38*, 245.
- [17] L. Gong, I. A. Kinloch, R. J. Young, I. Riaz, R. Jalil, K. S. Novoselov, *Adv. Mater.* **2010**, *22*, 2694.
- [18] W. E, B. Engquist, Z. Huang, *Phys. Rev. B* **2003**, *67*, 092101.
- [19] M. Vassaux, R. A. Richardson, P. V. Coveney, *Phil. Trans. R. Soc. A* **2018**, in press. <https://doi.org/10.1098/rsta.2018.0150>
- [20] W. Bangerth, R. Hartmann, G. Kanschat, *ACM Trans. Math. Softw.* **2007**, *33*.
- [21] S. Güryel, M. Walker, P. Geerlings, F. D. Proft, M. R. Wilson, *Phys. Chem. Chem. Phys.* **2017**, *19*, 12959.
- [22] S. Keten, Z. Xu, B. Ihle, M. J. Buehler, *Nat. Mater.* **2010**, *9*, 359.
- [23] J. L. Suter, D. Groen, P. V. Coveney, *Adv. Mater.* **2015**, *27*, 966.